A large amount synthesis of nanopowder using modulated induction thermal plasmas synchronized with intermittent feeding of raw materials

メタデータ	言語: eng
	出版者:
	公開日: 2017-10-03
	キーワード (Ja):
	キーワード (En):
	作成者:
	メールアドレス:
	所属:
URL	http://hdl.handle.net/2297/34167

A large amount synthesis of nanopowder using modulated induction thermal plasmas synchronized with intermittent feeding of raw materials

Yasunori Tanaka, Tatsuya Tsuke, Weixuan Guo, Yoshihiko Uesugi, Tatsuo Ishijima, Shu Watanabe†, Keitaro Nakamura†

Faculty of Electrical and Computer Engineering, Kanazawa University, Kakuma, Kanazawa 920-1192, Japan

‡Research Center for Production & Technology, Nisshin Seifun Group Inc.,5-3-1 Tsurugaoka, Fujimino 356-8511, JAPAN

E-mail: `tanaka@ec.t.kanazawa-u.ac.jp`

Abstract.
   A large amount synthesis method for titanium dioxide (TiO_2) nanopowder is proposed by direct evaporation of titanium powders using Ar-O_2 pulse-modulated induction thermal plasma (PMITP). To realize a large amount synthesis of nanopowder, the PMITP method was combined with the intermittent and heavy load feeding of raw material powder, as well as the quenching gas injection. The intermittent powder feeding was synchronized with the modulation of the coil current sustaining the PMITP for complete evaporation of the injected powder. Synthesized particles by the developed method were analyzed by FE-SEM and XRD. Results indicated that the synthesized particles by the 20-kW PMITP with a heavy loading rate of 12.3 g min^{-1} had a similar particle size distribution with the mean diameter about 40 nm to those with light loading of 4.2 g min^{-1}.

1. Introduction

The inductively coupled thermal plasmas (ICTPs) have been widely adopted as effective heat and chemical species sources for various materials processings such as syntheses of diamond films [1], thermal barrier coatings [2], fullerene synthesis [3], and surface modifications, etc [4]. The ICTP has some advantages like their high enthalpy and high radical density without any contamination. The ICTP is also useful to synthesize nanoparticles of various kinds [5]–[13]. It provides one-step direct processing including rapid evaporation of raw materials injected, and rapid cooling of evaporated materials. It can also offer nanoparticles in non-equilibrium or metastable phase [7, 8]. However, there are some issues about difficulty in controlling synthesized particle size and phase constituent. In addition, the production rate was relatively low compared to liquid phase synthesis for industrial application [14]. A large amount production method of nanopowder is thus strongly desired for future demand in nanotechnology fields.

On the other hand, the authors previously developed some series of modulated induction thermal plasma system including a pulse-modulated induction thermal plasmas (PMITP) system and an arbitrary-waveform-modulated induction thermal plasma (AMITP) system [15, 16]. The PMITP and AMITP are established by the coil current modulated into a rectangular or other

waveforms. Such a millisecond modulation can perturb the thermal plasma markedly, and then it can change the temperature and radical densities as well as the gas flow field in the thermal plasma in time domain [15]. Through this modulation, the temperature and radical densities can be controlled intentionally. We found actually that the Ar-N_2 PMITP provides simultaneous control of the nitrogen radical flow and the enthalpy flow for surface modification [17].

We have also studied to adopt the Ar-O_2 PMITP to nanoparticle synthesis of titanium dioxide (TiO_2). The TiO_2 nanoparticles in anatase phase are continuously receiving attention for use as photocatalysts [18], photonic crystals [19], photovoltaic cells [20], gas sensors [21], and a strong deoxidation material used for producing hydrogen gas from water for fuel cells [22]. The rutile type of TiO_2 is also useful mainly to pigment, cosmetic and medical powder due to its UV cut properties [23] , and to electronics material because of its higher dielectric constant and electrical resistance [24]. In our previous works, we have found that the modulation of the coil current can control the size of synthesized nanoparticles, while keeping the weight fraction of anatase-TiO_2 in synthesized nanoparticles to be about 85%–90% almost independent of the modulation condition [25]. It was also found that the size of synthesized nanoparticles depends on the temperature decay rate in the cooling period in the PMITP [26]. Our another work has developed a system for intermittent feeding of raw materials and studied the influence of the intermittent feeding fundamentally [27].

In this paper, we newly propose a large amount synthesis method of nanopowder using the PMITP. For a large amount synthesis of nanopowder, the PMITP was combined with intermittent heavy rate feeding of raw material, and also the quenching gas injection. Raw materials were fed to the PMITP only during the on-time for their efficient evaporation, and were stopped during the off-time for efficient cooling of the vapor by the quenching gas. Synthesized particles were analyzed by the field emission scanning electron microscopy (FE-SEM) and X-Ray Diffraction (XRD). Results indicated that the synthesized particles by the 20-kW PMITP with a heavy loading rate of 12.3 g min^{-1} had a particle size distribution with the mean diameter about 40 nm and the coefficient of variation of 0.53. This distribution was similar to those with light loading of 4.2 g min^{-1}.

2. Concept of a large amount synthesis of nanoparticles using modulated induction plasmas

Our previous work has studied the influence of coil current modulation of PMITP on the synthesized nanoparticles [26]. The PMITP can repetitively produce a high-temperature field during the 'on-time' and a low-temperature field during the 'off-time' in thermal plasmas. Here, the on-time means the time period with the higher current level (HCL), while the off-time is the time period with the lower current level (LCL). It was found from the experiments that a larger modulation degree in the coil current, which means a larger difference between HCL and LCL, decreased the mean diameter of the synthesized nanoparticles [26]. This means that the size of synthesized nanoparticle can be controlled by the shimmer current level (SCL) which is defined as a ratio of LCL to HCL, that is SCL=LCL/HCL. Our next step was concerned with the intermittent powder feeding effect on the synthesized nanoparticles [27]. That result indicated that particle size depended on the timing of the powder intermittent feeding, and that the size was smallest when the powder feeding timing was synchronized with the coil current modulation of the PMITP.

In this paper, we newly propose a method combined with the above methods for a large amount synthesis of nanopowder: the PMITP with intermittent feeding of raw material, and also the quenching gas injection. Figure 1 illustrates a comparison between (a) the conventional method using a non-modulated ICTP with continuous powder feeding, and (b) the proposed method using the PMITP with intermittent powder feeding method for a large amount of nanopowder production. In the conventional method, the raw material powder is continuously
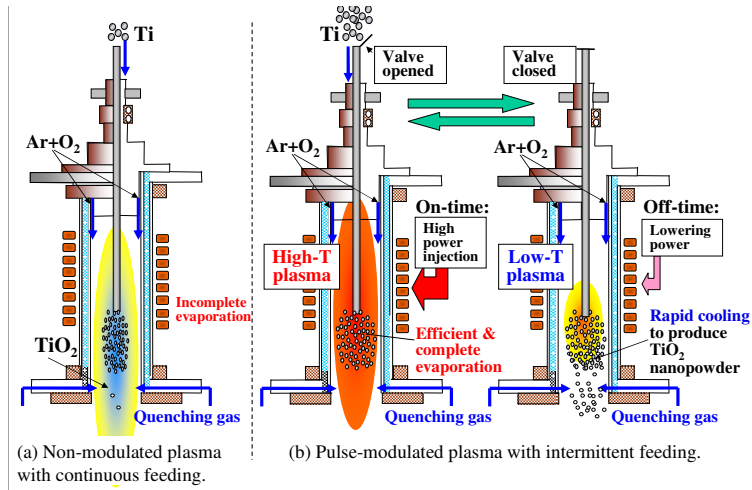
Figure 1. Concept of intermittent feeding of raw material.

fed directly to the ICTP. The ICTP evaporates the injected powder, and then the evaporated material is cooled down by the quenching gas downstream of the torch to create nanoparticles. However, the increasing powder feed rate causes a temperature drop around the center of the ICTP mainly for required latent heat of the material evaporation. Thus, the ICTP cannot completely evaporate the powders injected at heavy rate power feeding rate.

The proposed method uses the PMITP and the intermittent powder feeding technique. A high-speed solenoid valve is installed on the powder feeding tube for intermittent powder feeding. Setting the open and/or close timing of the valve controls the timing and duration of powder feeding. Thus, the developed method can make raw materials powder fed to the PMITP only during the on-time, and stopped during the off-time in the PMITP. In the on-time of the PMITP, the instantaneous input power to the plasma increases, and then it elevates the plasma temperature. Therefore, the injected powder can be evaporated efficiently and completely in the PMITP. On the other hand, in the off-time of the PMITP, the input power decreases to decay the plasma temperature in milliseconds. Meanwhile, the powder feeding is stopped by closing the valve. Thus, the above evaporated materials are efficiently cooled down during this time. In addition, this cool-down efficiency of the evaporated materials is promoted by the quenching gas injected into downstream of the plasma torch. The Ti atom and oxygen atom are cooled down to produce TiO molecules in gas phase, and then nucleation of TiO_2 may occur before nucleation of Ti [11]. After that, TiO_2 condensation, and agglomeration may take place until coagulation.

3. Experimental

3.1. Experimental arrangements

Figure 2 shows the whole nanoparticle synthesis system using the PMITP used in the present work. This whole system has three parts: the rf power source, intermittent powder feeding system, and the plasma torch and the chambers.

The rf power source is operated with a metal-oxide semiconductor field emission transistor (MOSFET) at rated power of 30 kW. This power source can modulate the electric current amplitude of several hundreds of amperes into a rectangular waveform in this work. The modulated coil current has modulation parameters such as the on-time, and the off-time as indicated in the previous section [15]. The shimmer current level (SCL) is defined as LCL/HCL,
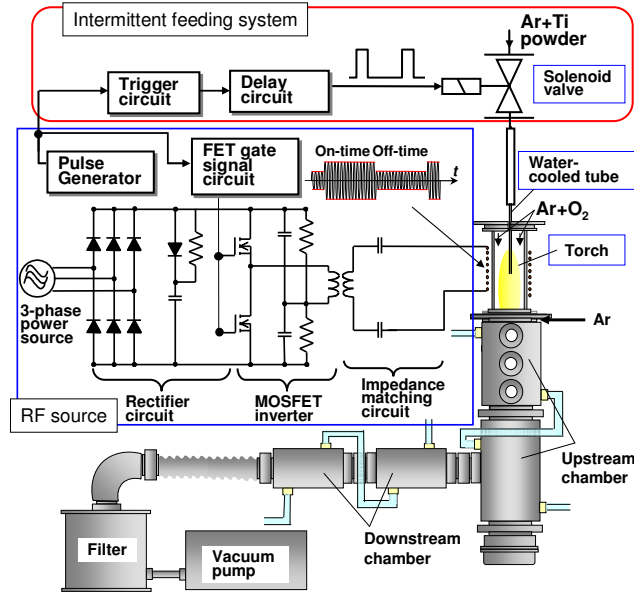
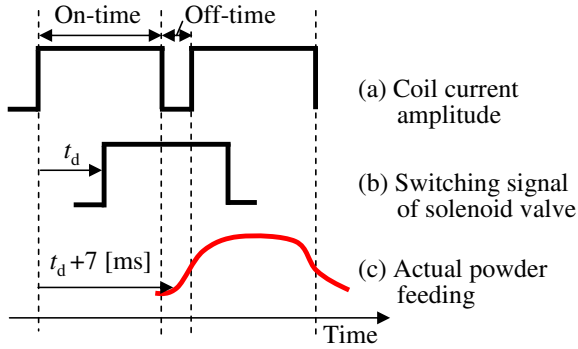**Figure 2.** System for intermittent feeding of raw material.

Figure 3. Timing chart in feeding of raw material.

which is often used in the experiment. In addition, the duty factor (DF) is set to a ratio of the on-time to one modulation cycle: DF= 'on-time' /('on-time' +'off-time').

The plasma torch and the chambers in Fig. 2 are configured identically to that used in our previous work [25, 26]. The plasma torch has two coaxial quartz tubes. The inner diameter of the interior quartz tube is 70 mm; its length is 370 mm. Into the plasma torch, a water-cooled tube for powder feeding is inserted from the plasma torch head. Downstream of the plasma torch, quenching gas can be injected in radial direction from eight holes installed on the flange. Further downstream has the water-cooled chambers, separately named as the upstream chamber and the downstream chamber, which are respectively installed in vertical and then in horizontal, as depicted in Fig. 2. Finally, a powder-collecting filter is set up and then a vacuum pump.

The upper side in Fig. 2 portrays the system for intermittent feeding of raw material to the PMITP. The system contains the trigger circuit, the delay circuit and a high speed solenoid valve. The pulse generator in the rf source provides the modulation control signal with 0–10 V to the FET gate signal circuit and also to the trigger circuit in the intermittent feeding system. The FET gate signal circuit controls the fire angle of the MOSFET elements for rf power supply and also for the amplitude modulation of the coil current. On the other hand, the trigger circuit and then the delay circuit controls the opening and closing of a high-speed solenoid valve. This

Table 1. Experimental condition.

Time-averaged input power	20 kW
Fundamental frequency of the coil current	450 kHz
Modulation cycle	15 ms
Shimmer current level, SCL	60%[a] or 80%[b]
Duty factor, DF	80% (On-time / Off-time=12 ms / 3 ms)
Pressure	300 torr (= 40 kPa)
Gas composition	Ar:90 L min^{-1},O$_2$:10 L min^{-1}
Carrier gas flow rate	Ar:4 L min^{-1}
Quenching gas flow rate	Ar:50 L min^{-1}
Delay time of solenoid valve open t_{d}	6 ms
Powder feed rate g_{pow}	12.3 g min^{-1}[a] or 4.2 g min^{-1}[b]
Raw powder and its maximum size	Ti, 45 μm

a. SCL=60% for g_{pow}=12.3 g min^{-1}
b. SCL=80% for g_{pow}=4.2 g min^{-1}

solenoid valve has a response time constant of less than 2 ms. Use of this system enables us to intermittently feed the raw material powder to the thermal plasma with controlling feed timing.

Figure 3 schematically illustrates the timing chart of (a) the coil current amplitude, (b) the switching signal of solenoid valve, and (c) the actual powder feeding. The coil current amplitude was assumed to change from LCL to HCL at a certain timing t=0 ms. By using the current modulation signal, the signal in the TTL level was created in the trigger circuit to the delay circuit. The delay circuit outputs a signal with the delay time t_{d} against the current modulation signal to open the valve. After opening the solenoid valve, the powder was supplied actually with another delay time t_{adt} because the distance between the valve and the tip of the water-cool tube is about 870 mm long. This delay time t_{adt} has been measured to be $6-8$ ms by spectroscopic observation in our previous work [26] Thus, there is the actual total delay time of $t_{\mathrm{d}} + t_{\mathrm{adt}} \sim t_{\mathrm{d}} + 7$ ms before the powder is actually injected from the tip of the water-cooled tube. Controlling t_{d} makes it possible to change the timing of powder injection intentionally. The powder can be controlled to be supplied only during the on-time of the PMITP.

3.2. Experimental conditions
Table 1 summarizes the experimental condition in the present work. The time-averaged input power was fixed at 20 kW to the inverter power supply. This inverter power supply in the experiment was a semiconductor power supply with a fundamental frequency of 450 kHz. This power supply was measured to have a high power conversion efficiency more than 95%. Thus, the more than 19 kW was outputed from the power supply. The instantaneous input power $P_{\mathrm{in}}(t)$ was also periodically changes with time according to the coil current modulation. For 80%SCL-80%DF, the quantity $P_{\mathrm{in}}(t)$ increased gradually with time constant about 1.6 ms during the on-time and reached to 28 kW, whereas it decreased with time constant of 2.0 ms in the off-time, reaching to 10 kW. The modulation cycle was fixed at 15 ms. The reason to select the modulation cycle of 15 ms is attributed to the fact that the residence time of the reactant vapor was estimated as 10–20 ms according to the gas flow velocity calculation by numerical

thermofluid simulation [25]. It is expected to provide sufficient evaporation of the injected powders in the high-temperature region in the plasma during the on-time, and successive rapid cooling of the plasma tail during the off-time. The DF of the modulated coil current was fixed at 80%. The SCL was set to 60% or 80%.

The total flow rate of Ar-O_2 sheath gas was fixed at 100.0 L min^{-1} (liters per minute). The oxygen gas admixture ratio to Ar was 10% in the sheath gas in the gas flow rate. The gas flow rate of Ar carrier gas was 4 L min^{-1}. Titanium powder with maximum diameter of 45 μm and with mean diameter of 27 μm is fed as the raw material together with Ar carrier gas. The powder was injected through a water-cooled tube probe made of stainless steel. The powder feed rate g_{pow} of the Ti raw material was set at 4.2 g min^{-1} (=7.0 × 10^{-5} kg s^{-1}), and also at 12.3 g min^{-1} (=21 × 10^{-5} kg s^{-1}) as a heavy load feeding condition for nanopowder mass production. The magnitude of this powder feed rate was time-averaged value which is determined as follows: the weight w_1 [g] of Ti raw material powder in the powder feeder was measured before the experiment, and then the weight w_2 [g] of Ti raw material powder in the powder feeder was also measured after the experiment. The time-averaged value of the powder feed rate was calculated as $(w_1 - w_2)/t_{exp}$ where t_{exp} is the experiment time. The definition of the time-averaged feeding rate is necessary because the actual instantaneous feeding rate changes with time by opening and closing the valve intermittently in the present work. Note that powder feeding rate of g_{pow}=12.3 g min^{-1} at 20 kW that we used here is eminently a larger amount among the conventional ICTP nanopowder synthesis methods. The conventional methods usually use the rate of 1–4 g min^{-1} for 20–30 kW. Note that the powder feed rate of g_{pow}=12.3 g min^{-1} requires 2.3 kW for heating Ti bulk from 300 K through complete melting to complete evaporation.

As described in the previous section, a high-speed solenoid valve was installed on the powder feeding tube for intermittent powder feeding. The response time of the solenoid valve was about 2 ms. The delay time t_d of the valve open signal was set to 6 ms against the signal. In this case, the powder is initiated to be supplied at about 13 ms after the current transition from LCL to HCL. This timing corresponds to the synchronized timing of powder feeding with the next on-time of the coil current [27].

Argon quenching gas was injected downstream of the torch in radial direction with a gas flow rate of 50 L min^{-1}. The pressure inside the chamber was controlled at 300 Torr (=40 kPa) with an automatic feedback control for pressure. Synthesized particles were collected in the upstream chamber and the downstream chamber, and in the collecting filter.

4. Results for a heavy rate production of nanoparticles

4.1. SEM images and particle size distribution

Figure 4 presents examples of FE-SEM micrographs of particles synthesized using the PMITP with intermittent powder feeding. The powder feed rate g_{pow} was 12.3 g min^{-1}, i.e., a heavy rate injection. For comparison, those for g_{pow}=4.2 g min^{-1} are also indicated in Fig. 5. Panel (a) in these figures portrays the image for particles collected in the upstream chamber, whereas panel (b) shows the one in the collecting filter. The collecting yields were both about 0.5–0.6. As seen in these figures, particles for g_{pow}=12.3 g min^{-1} generally have larger sizes than those g_{pow}=4.2 g min^{-1}. Nevertheless, an important point is that even a heavy rate feeding condition g_{pow}=12.3 g min^{-1} could provide many nanoparticles with diameter sizes less than 100 nm.

Figures 6 and 7 show the particle size distributions for g_{pow}=12.3 g min^{-1} and g_{pow}=4.2 g min^{-1}, respectively. Similarly, panel (a) in these figures portrays the result for particles collected in the upstream chamber, whereas panel (b) shows the one in the collecting filter. These size distributions were obtained from 200 randomly sampled particles in the micrographs in Figs. 4 and 5. These figures also include the cumulative fraction, the mean diameter $\bar{d}$, the median diameter d_{50} and the standard deviation σ.
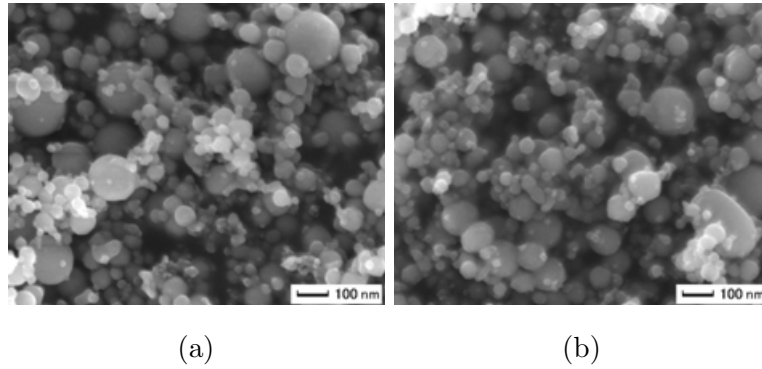
(a)   (b)

Figure 4. SEM picture of fabricated particle in large amount powder feeding. Powder feed rate was set to 12.3 g/min. (a), Upstream chamber ; (b), Filter.
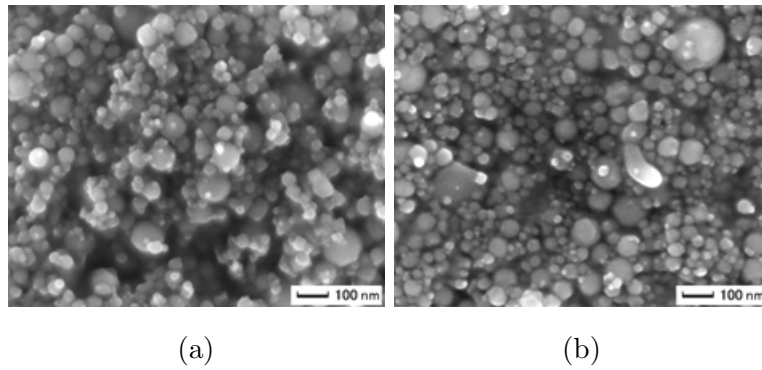

(a)   (b)

Figure 5. SEM picture of fabricated particle in little amount powder feeding. Powder feed rate was set to 4.2 g/min.(a), Upstream chamber ; (b), Filter.

For g_{pow}=4.2 g min^{-1}, the $\bar{d}$ is about $32-33$ nm irrespective of the powder collection position. This independence of the collection position means that the cooling effect from the quenching gas was enough for creation of nanoparticles from a small amount of Ti vapor. The standard deviation σ of $16-17$ nm is relatively low. On the other hand, for g_{pow}=12.3 g min^{-1}, $\bar{d}$ and σ depend on the collection position. The particles collected in the filter have larger $\bar{d}$ of 42.5 nm and σ of 22.5 nm. The dependence of the collection position is considered to arise from the cooling history of the material vapor. The particles collected in the upstream chamber are regarded as the ones fabricated by rapid cooling of the mixture of Ti and oxygen atoms directly on the short distance to the chamber wall. The rapid cooling generally prevents the particles from growing up due to coagulation. From this reason, the smaller nanoparticles might be obtained in the upper chamber. In the meanwhile, the particles collected in the filter are regarded as the ones created around the axis of the chamber which is transferred to the filter on the long way. The cooling rate for the mixture of Ti and oxygen atoms is relatively low compared to the above situation, and then the particles grow up in size. Hence, the relatively large particles may be found in this case. Nevertheless, the most particles are limited in size smaller than 100 nm, i.e. the nanoparticle size even for the heavy rate injection of Ti raw material. The coefficient of variation $\sigma/\bar{d}$ is $0.52-0.53$ for both cases g_{pow}=4.2 g min^{-1} and 12.3 g min^{-1}.

4.2. XRD spectra and weight fraction of anatase and rutile TiO$_2$

The TiO$_2$ has mainly three phases in the structure: rutile, anatase and brookite. Such crystallographic structure and chemical composition of the synthesized nanoparticles were investigated using XRD analysis. Figures 8 and 9 represent the XRD spectra for $g_{\rm pow}$=12.3 g min^{-1} and $g_{\rm pow}$=4.2 g min^{-1}, respectively. Again, panel (a) portrays the image for particles collected in the upstream chamber, whereas panel (b) is the one in the collecting filter. The XRD spectra weakly depend on the powder collection position for both powder feed rate conditions. This implies that cooling rate hardly influenced the crystallographic structure but oxygen content did it in the present conditions as described later. What should be emphasized here is that there is no peak from Ti raw material even in case of the heavy rate injection. The fact of no Ti peak indicates that injected Ti powder was completely evaporated and oxidized in the PMITP for $g_{\rm pow}$=12.3 g min^{-1} as well as $g_{\rm pow}$=4.2 g min^{-1}. Another noticeable fact is that there is quite a difference in results between Fig. 8 and Fig. 9. The particles for $g_{\rm pow}$=12.3 g min^{-1} indicates many peaks from the rutile phase as designated by 'R'. On the other hand, the dominant peaks from the particles for $g_{\rm pow}$=4.2 g min^{-1} are due to the metastable anatase phase denoted by 'A'. This difference may be attributed to the oxygen amount against Ti vapor as described later.

Calculating the ratio of the XRD intensity for these spectral lines, we estimated the weight fraction $f_{\rm A}$ of TiO$_2$ in anatase form to whole TiO$_2$ particles using the method indicated in [13, 25]:

$$f_{\rm A} = \frac{1}{1 + 1.26\dfrac{I_{\rm R_{27.4^o}}}{I_{\rm A_{25.3^o}}}}, \tag{1}$$

where $I_{\rm R_{27.4^o}}$ and $I_{\rm A_{25.3^o}}$ respectively signify the XRD spectral intensities at 2θ=27.4^o for rutile and 2θ=25.3^o for anatase. This equation was obtained using the test line for standard TiO$_2$. Figure 10 presents the weight fraction of anatase TiO$_2$ to whole TiO$_2$ particles for different powder collection positions for two $g_{\rm pow}$ conditions. The weight fraction of anatase TiO$_2$ is a high value of 0.84 for $g_{\rm pow}$=4.2 g min^{-1}, almost irrespective of the powder collection position. On the other hand, the weight fraction is about 0.35 for $g_{\rm pow}$=12.3 g min^{-1}. In other words, 0.65 of the whole particles are in rutile phase. This difference may be explained by oxygen amount as described in literature [9]. They had showed experimentally that the phase composition of the TiO$_2$ nanoparticles from the solidification of vaporized species depends on the ambient oxygen concentration. They also deduced that the weight fraction of anatase-TiO$_2$ could be increased by increasing oxygen gas flow rate, because rutile TiO$_2$ tends to be solidified from oxygen-deficient clusters while anatase TiO$_2$ inclines to be obtained from oxygen-rich clusters [9]. According to their results, the oxygen amount in the present work was too low to obtain anatase-TiO$_2$ for a large amount of powder feed rate $g_{\rm pow}$=12.3 g min^{-1}, while it was enough for $g_{\rm pow}$=4.2 g min^{-1}. The weight fraction of anatase-TiO$_2$ could be expected to be improved by more oxygen gas injection.

5. Conclusions

This paper has proposed a new method for a large amount synthesis of TiO$_2$ nanopowder using the Ar-O$_2$ PMITP with an intermittent heavy rate powder feeding and quenching gas injection. Ti raw material powder was intermittently injected into the PMITP only during the on-time, synchronized with the coil current modulation. This synchronized intermittent powder feeding with a rate of 12.3 g min^{-1} offered complete evaporation of Ti powder in the 20-kW PMITP. The evaporated materials were rapidly cooled down to create nanoparticles by quenching gas injection. Synthesized particles were analyzed by SEM and XRD. Results indicated that almost all particles were TiO$_2$, no Ti remaining. The mean diameter and standard deviation were 40 nm and 21 nm, respectively, for a feed rate condition of 12.3 g min^{-1}.
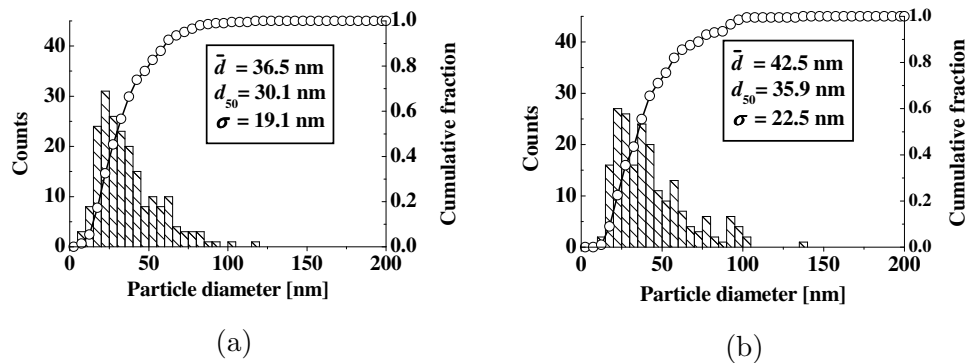
Figure 6. Size distribution of fabricated particle in large amount powder feeding. Powder feed rate was set to 12.3 g/min. (a), Upstream chamber ; (b) Filter.
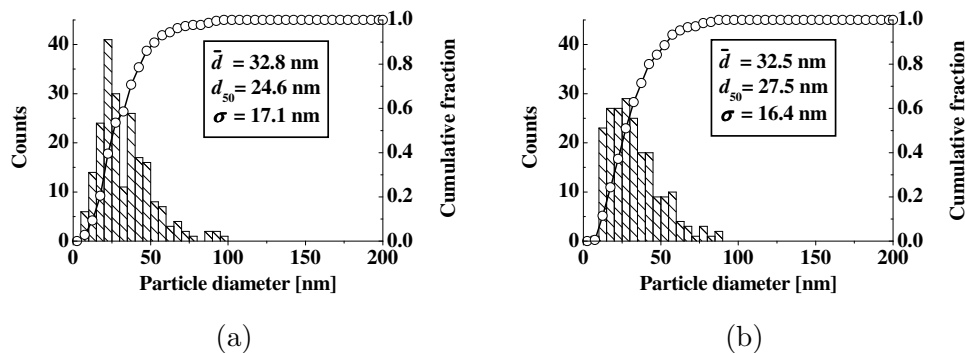

Figure 7. Size distribution of fabricated particle in large amount powder feeding. Powder feed rate was set to 4.2 g/min. (a), Upstream chamber ; (b) Filter.
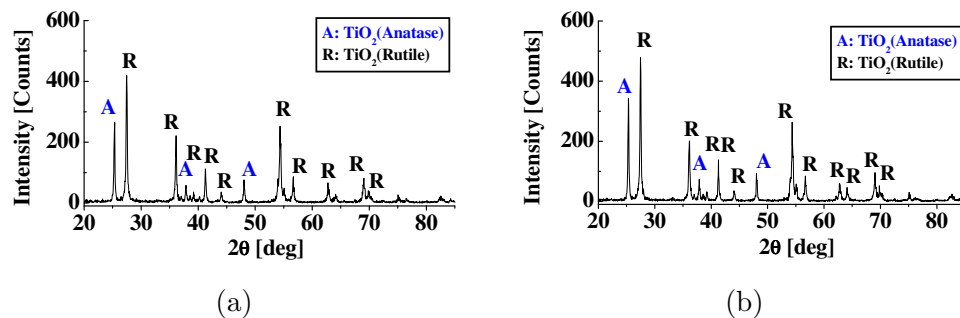

Figure 8. XRD spectra of fabricated particle in large amount powder feeding. Powder feed rate was set to 12.3 g/min. (a), Upstream chamber ; (b) Filter.

References

[1] Berghaus J O, Meunier J L and Gitzhofer F 2004 *Meas. Sci. Technol.* **15** 161
[2] Chen W R, Wu X, Marple B R and Patnaik P C 2005 *Surface & Coatings Technol.* **197** 109
[3] Wang C, Inazaki A, Shirai T, Tanaka Y, Sakuta T, Takikawa H and Matsuo H 2003 *Thin Solid Films* **425** 41
[4] Tanaka H, Osawa T, Moriyoshi Y, Kurihara M, Maruyama S and Ishigaki T 2004 *Thin Solid Films* **457** 209
[5] Shigeta M and Watanabe T 2010 *J. Appl. Phys.* **108** 043306
[6] Chen L C 2010 *J.Alloys & Compounds*, **495** 476
[7] Li Y and Ishigaki T 2002 *J. Cryst. Growth* **242** 511
[8] Huang J Y, Ishigaki T, Tanaka T and Horiuchi S 1998 *J. Mater. Sci.* **33** 4141
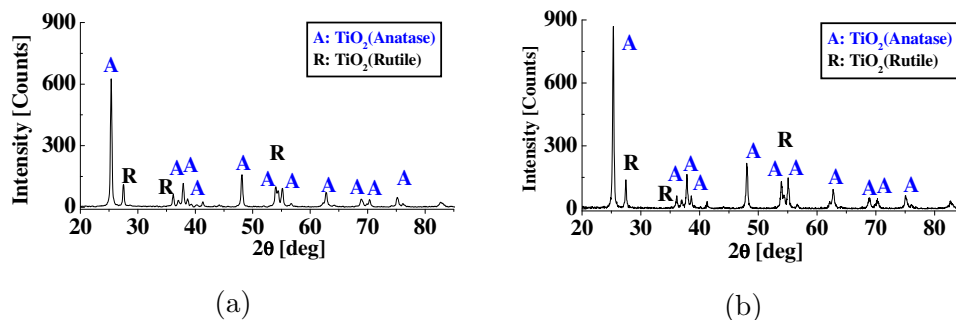
Figure 9. XRD spectra of fabricated particle in large amount powder feeding. Powder feed rate was set to 4.2 g/min. (a), Upstream chamber ; (b) Filter.
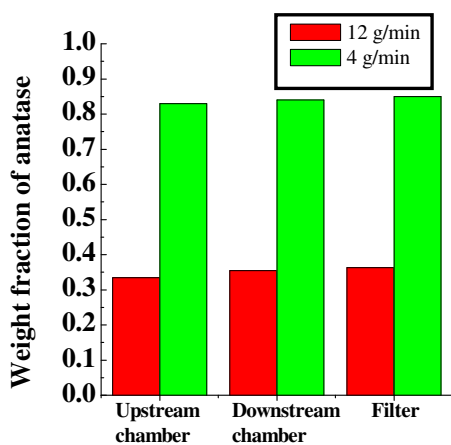

Figure 10. Weight fraction of TiO_2 in anatase phase in the fabricated nanoparticles.

 [9] Oh S M and Ishigaki T 2004 *Thin Solid Films* **457** 186
[10] Lee J E, Oh S M and Park D W 2004 *Thin Solid Films* **457** 230
[11] Watanabe T and Fujiwara K 2004 *Chem. Eng. Comm.* **191** 1343
[12] Ishigaki T and Li J G 2007 *Sci. & Technol. Advanced Mater.* **8** 617
[13] Li J G, Ikeda M, Ye R, Moriyoshi Y and Ishigaki T 2007 *J. Phys. D: Appl. Phys.* **40** 2348
[14] Chen X and Mao S S 2007 *Chem. Rev.* **107** Issue 7, 2891
[15] Tanaka Y, Uesugi Y, Sakuta T 2007 *Plasma Sources Sci. & Technol.* **16** 281
[16] Tanaka Y, Morishita Y, Okunaga K, Fushie S and Uesugi Y 2007 *Appl. Phys. Lett.* **90** 071502
[17] Tanaka Y, Hayashi K, Nakamura T and Uesugi Y 2008 *J. Phys. D: Appl. Phys.* **41** 185203
[18] Malato S, Blanco J, Alarcon D C, Maldonado M I, Fernandez-Ibanez P and Gernjak W 2007 *Catalysis Today* **122** 137
[19] Li J, Zhao X, Wei H, Gu Z Z, Lu Z 2008 *Analytica Chemica Acta* **625** 63
[20] Gratzel M 2001 *Nature* **414** 338
[21] Biju K P, Jain M K 2008 *Thin Solid Films* **516** 2175
[22] Park J H, Park O O and Kim S 2006 *Appl. Phys. Lett.* **89** 163106
[23] Lee K N, Kim Y, Lee C W and Jai-Sung Lee J S 2011 *Mater. Sci. Eng.* **18** 082021
[24] Liu P S, Cai W P, Wan L X, Shi M D, Luo X D and Jing W P 2009 *Trans. Nonferrous Met. Soc. China* **19** s743
[25] Tanaka Y, Nagumo T, Sakai H, Uesugi Y, Sakai Y and Nakamura K 2010 *J. Phys. D: Appl. Phys.* **43** 265201
[26] Tanaka Y, Sakai H, Tsuke T, Uesugi Y, Sakai Y and Nakamura K 2011 *Thin Solid Films* **519** Issue 20, 7100
[27] Tanaka Y, Sakai H, Tsuke T, Guo W, Uesugi Y, Sakai Y and Nakamura K 2011 *Proc. 20th Int. Symp. Plasma Chem. ISPC-20*, 346, Philadelphia, USA